Parameter Estimation of Transient Multiexponential Signals Using SVD–ARMA and Multiparameter Deconvolution Techniques

2 authors:

Abdussamad Jibia
Bayero University, Kano
17 PUBLICATIONS   **44** CITATIONS

SEE PROFILE

Momoh Salami
International Islamic University Malaysia
140 PUBLICATIONS   **934** CITATIONS

SEE PROFILE

Some of the authors of this publication are also working on these related projects:

Control strategies for positioning systems View project

Decision Making in Cognitive Radio: Automatic Threshold Estimation View project

Parameter Estimation of Transient Multiexponential Signals Using SVD-ARMA and Multiparameter Deconvolution Techniques

Abdussamad U. Jibia and Momoh-Jimoh E. Salami

Abstract—**Much has been reported about the analysis of transient multiexponentials data. In a previous paper, for example, this analysis was done using autoregressive moving average model which was applied to the deconvolved data arising from the application of Gardner transform followed by optimal compensation deconvolution to the original signal. Optimal compensation deconvolution uses a single parameter noise-reduction parameter. In this paper, a deconvolution parameter incorporating multiple noise-reduction parameters is used instead. Simulations and experimental results show that the proposed combination, despite its limitations supersedes several existing methods.**

Index Terms—**ARMA, multiparameter, multiexponential, deconvolution.**

I. INTRODUCTION

Problems involving the analysis of multiexponential transient data with real decay rates are common in Applied Physics and Chemistry. Examples are fluorescence decay analysis in biophysics, radioactive decay in nuclear Physics and reaction kinetics in Chemistry. The mathematical representation of such signals is given in (1).

$$S(\tau) = \sum_{i=1}^{M} A_i \exp(-\lambda_i \tau) + n(\tau) \quad 0 < \tau < \infty \quad (1)$$

This signal is measured and the number of components, M, preexponential factors, A_i and the decay rates, λ_i are estimated.

Three reasons make the solution of this problem difficult. A series of nonlinear equations is involved, the available data only approximates the function $S(\tau)$ over a finite range in τ and the nonorthogonality of exponentially decaying functions.

Several techniques have been used for this analysis (see for example [1] and [2]). The methods differ according to speed, computational simplicity, accuracy and the existence or lack of initial approximations, among other differences. In a previous paper [3], this analysis was done by means of Gardner transform which was used to convert the signal in (1) into a convolution integral which was discretized and

deconvolved using optimal compensation deconvolution method. The deconvolved data was then further processed using autoregressive moving average (ARMA) model whose AR parameters were determined by solving high order Yule-Walker equations via singular value decomposition (SVD) algorithm. Optimal compensation deconvolution is essentially conventional inverse filtering with a single noise-reduction parameter introduced. In this paper, the approach in [3] is modified by using multiparameter deconvolution technique. The use of multiple deconvolution parameters is not new even though our use of it in combination with ARMA model is novel. The particular approach we use here was originally proposed by Daboczi and Kollar [4] and generalized by Zhang et al [5]. The Zhang's model is modified and applied in this analysis. Specifically, only two parameters are used and all others suppressed. Another improvement over the approach in [3] is the fact that whereas in [3] the truncation point of the deconvolved data was determined by trial and adjustment, in this paper Cramer Rao Lower Bound as derived and used in [6, 7] is used to determine the good length of the deconvolved data. A number of simulations were carried out to test the efficacy of the proposed combination using different synthetic signals.

It is shown through simulations and experiments that this combination outperforms many existing methods. It is however not without its limitations.

II. DEVELOPMENT OF A CONVOLUTION SUM

In this section, Gardner transform is applied to convert the original signal in (1) into a convolution model hence removing the nonorthogonality problem associated with the signal.

Eq. (1) can be expressed as follows:

$$S(\tau) = \int_{0}^{\infty} g(\lambda) \exp(-\lambda \tau) d\lambda + n(\tau) \quad (2)$$

where

$$g(\lambda) = \sum_{i=1}^{M} A_i \delta(\lambda - \lambda_i) \quad (3)$$

The integral in (2) belongs to the more general class of Fredholm integral of the first kind which are known to be

ill-posed. This term means that the solution of (2) may not be unique, may not exist, and may not depend continuously on the data.

Multiplying both sides of (2) by τ^α, $\alpha > 0$ and applying the Gardner transform [8], $\tau = e^t$ and $\lambda = e^{-r}$ results in the convolution integral

$$y(t) = \int_{-\infty}^{\infty} x(\lambda)h(t - \lambda)d\lambda + v(t) \tag{4}$$

where

$$y(t) = \exp(\alpha t)S(\exp(t)) \tag{5a}$$

$$x(t) = \exp((\alpha - 1)t)g(e^{-t}) \tag{5b}$$

$$h(t) = \exp(\alpha t)\exp(-e^t) \tag{5c}$$

$$v(t) = \exp(\alpha t)n(e^t) \tag{5d}$$

This is now a standard deconvolution problem in which $x(t)$ is the unknown input signal consisting of a series of weighted delta functions, $h(t)$ is the impulse response and $y(t)$ is the output observation.

It can be shown [9] that the unknown input distribution function is given by

$$x(t) = \sum_{i=1}^{M} B_i \delta(t + \ln \lambda_i) \tag{6}$$

where $B_i = A_i(\lambda_i)^{-\alpha}$

Eq. 4 can be converted to a discrete-time deconvolution model by sampling $y(t)$ at the rate of $f_s = \frac{1}{\Delta t}$. This yields

$$y[n] = \sum_{m=n_{\min}}^{n_{\max}} x[m]h[n - m] + v[n] \tag{7}$$

where $N = n_{\max} - n_{\min} + 1$ and the sampling interval is $\Delta t \le \frac{1}{\alpha}$.

III. SIGNAL MODELING

Deconvolution of the convolution sum of (7) is achieved by solving stabilized solutions of integral of the first kind.

$$\int_{\Lambda_1}^{\Lambda_2} x(\lambda)h(t, \lambda)d\lambda = Hx = y(t) \quad for\ T_1 < t < T_2 \tag{9}$$

We now select a space $F = W_2^q[\Lambda_1, \Lambda_2]$ and compute the square of the integrable functional form with derivatives of q order in the region of $[\Lambda_1, \Lambda_2]$.

The stable solutions $\hat{x}$ should make the following smoothing functional a minimum:

$$M^\beta[\hat{x}, y] = \|H\hat{x} - y\|^2 + \beta\Omega(\hat{x}) \tag{10}$$

where $M^\beta[\hat{x}, y]$ expresses smoothing function.

Now, if we take the stable functional

$$\Omega(\hat{x}) = \int_{\Lambda_1}^{\Lambda_2} \sum_{r=0}^{q} \xi_r (d^r \hat{x})^2 d\lambda \tag{11}$$

where ξ_r are selected known constants or functions of λ such that

$\xi_r \ge 0$ when $r = 0, 1, \dots, q-1$

and $\xi_r > 0$ when $r = q$

and $d^r\hat{x}$ is the expression of rth order derivative of $\hat{x}$.

$$M^\beta[\hat{x}, y] = \|H\hat{x} - y\|^2 + \beta\Omega(\hat{x})$$
$$= \|H\hat{x} - y\|^2 + \beta\int_{\Lambda_1}^{\Lambda_2}\sum_{r=0}^{q}\xi_r(d^r\hat{x})^2 d\lambda \tag{12}$$

In discrete form, this becomes

$$SM^\beta[\hat{x}(n), y(n)] = \sum_{n=0}^{N-1}\left[y(n) - \sum_{m=-n_{\min}}^{n_{\max}}h(m)\hat{x}(n-m)\right]^2$$
$$+ \beta\sum_{r=0}^{q}\sum_{n=0}^{N-1}\xi_r\left[\sum_{m=-n_{\min}}^{n_{\max}}\nabla^r\hat{x}(n-m)\right]^2 \tag{13}$$

where S denotes the sampling operation and ∇^r denotes the rth order backward difference operator since ∇ is the discrete analog of the derivative.

In the frequency domain:

$$SM^\beta[\hat{X}(k), Y(k)] = \frac{\Delta t}{N}\sum_{k=0}^{N-1}|Y(k) - H(k)\hat{X}(k)|^2$$
$$+ \frac{\Delta t}{N}\beta\sum_{r=0}^{q}\sum_{k=0}^{N-1}\xi_r|L_r(k)\hat{X}(k)|^2 \tag{14}$$

Thus,

$$SM^{\beta}\left[\hat{X}(k), Y(k)\right] =$$

$$\frac{\Delta t}{N} \sum_{k=0}^{N-1} \left\{ \begin{array}{l} \left[Y(k) - H(k)\hat{X}(k)\right] \\ \left[\begin{array}{l} Y^{*}(k) \\ -H^{*}(k)\hat{X}^{*}(k) \end{array}\right] \\ + \beta \sum_{r=0}^{q} \dfrac{\xi_{r} L(k)}{L^{*}(k)\hat{X}(k)\hat{X}^{*}(k)} \end{array} \right\}$$

$$= \frac{\Delta t}{N} \sum_{k=0}^{N-1} \left\{ \begin{array}{l} Y(k)Y^{*}(k) - \\ Y(k)H^{*}(k)\hat{X}^{*}(k) \\ - H(k)\hat{X}(k)Y^{*}(k) \\ + H(k)H^{*}(k) \\ \hat{X}(k)\hat{X}^{*}(k) \\ + \beta \sum_{r=0}^{q} \dfrac{\xi_{r} L(k)}{L^{*}(k)\hat{X}(k)\hat{X}^{*}(k)} \end{array} \right\} \quad (15)$$

$$\frac{\partial SM^{\beta}\left[\hat{X}(k), Y(k)\right]}{\partial \hat{X}(k)} =$$

$$\frac{\Delta t}{N} \sum_{k=0}^{N-1} \left\{ \begin{array}{l} |H(k)|^{2} X^{*}(k) \\ - Y^{*}(k)H(k) \\ + \beta \sum_{r=0}^{q} \xi_{r} |L_{r}(k)|^{2} \hat{X}^{*}(k) \end{array} \right\} \quad (16)$$

If $\dfrac{\partial SM^{\beta}\left[\hat{X}(k), Y(k)\right]}{\partial \hat{X}(k)} = 0$, then

$$\hat{X}^{*}(k) = \frac{Y^{*}(k)H(k)}{|H(k)|^{2} + \beta \sum_{r=0}^{q} \xi_{r} |L_{r}(k)|^{2}} \quad (17)$$

Taking the complex conjugate of both sides yields

$$\hat{X}(k) = \frac{Y(k)H^{*}(k)}{|H(k)|^{2} + \sum_{r=0}^{q} \delta_{r} |L_{r}(k)|^{2}} \quad (18)$$

$k = 0,1,2,.............N-1$ and $\delta_{r} = \beta \xi_{r}$.

The term $|L_{r}(k)|^{2}$ is derived as follows:

From equation (13), let

$$b_{r}(n) = \nabla^{r} x[n] \quad (19)$$

Then, for $r = 1$

$$b_{1}(n) = \nabla x(n) = x(n) - x(n-1) \quad (20)$$

So that

$$B_{1}(e^{j\omega}) = X(e^{j\omega})(1 - e^{j\omega}) \quad (21)$$

Let $L_{1}(e^{j\omega}) = \dfrac{B_{1}(e^{j\omega})}{X(e^{j\omega})} = \left(1 - e^{j\omega}\right) \quad (22)$

For DFT/FFT analysis

Taking $\omega_{k} = \dfrac{2\pi k}{N}$ yields

$$L_{1}(k) = 1 - e^{-j\frac{2\pi k}{N}} = 2j \sin\frac{\pi k}{N} e^{-j\frac{2\pi k}{N}} \quad (23)$$

$$\Rightarrow |L_{1}(k)|^{2} = 4\sin^{2}\left(\frac{\pi k}{N}\right) \quad (24)$$

Similarly, for $r = 2$

$$L_{2}(e^{j\omega}) = \frac{B_{2}(e^{j\omega})}{X(e^{j\omega})} = -4e^{-j\omega}\left(\frac{e^{\frac{j\omega}{2}} - e^{-\frac{j\omega}{2}}}{2j}\right)^{2} \quad (25)$$

With $\omega = \dfrac{2\pi k}{N}$, we have

$$L_{2}(k) = -4e^{-j\frac{2\pi k}{N}}\left(\sin^{2}\left(\frac{\pi k}{N}\right)\right) \quad (26)$$

Hence,

$$|L_{2}(k)|^{2} = 16\sin^{4}\left(\frac{\pi k}{N}\right) \quad (27)$$

It is therefore observed that Daboczi multiparameter optimization model [4] is a special case of the generalized multiparameter deconvolution where $|L_{r}(k)|^{2}$ can be progressively used to improve the SNR of the deconvolved data. Consequently, if needed, we can find $|L_{r}(k)|^{2}$ for any r.

In this paper, the following model is used

$$\hat{X}(k) = \frac{Y(k)H^{*}(k)}{|H(k)|^{2} + \varsigma |L_{1}(k)|^{2} + \gamma |L_{2}(k)|^{2}} \quad (28)$$

This is exactly the model of equation (18) with $q = 2$, $\delta_{0} = 0$, $\delta_{1} = \varsigma$ and $\delta_{2} = \gamma$.

The estimated input distribution in (6) is computed by Fourier transformation which gives

$$\hat{X}(k) = \sum_{i=1}^{M} B_i e^{j\frac{2\pi k}{N}\ln \lambda_i} \qquad (29)$$

The output of the deconvolution stage will take this form. However, when the additive noise component $n(\tau)$ is considered, the signal will contain a nonstationary noise component, $\varepsilon(k)$ as follows:

$$\hat{X}(k) = \sum_{i=1}^{M} B_i e^{j\frac{2\pi k}{N}\ln \lambda_i} + \varepsilon(k) \qquad (30)$$

The noise $\varepsilon(k)$ is different from the original noise $n(\tau)$ and the $v(t)$ in (4). This is because the original signal $S(\tau)$ has undergone many manipulations including Gardner transformation, discretization and deconvolution, to arrive at (30). Therefore even if $n(\tau)$ is stationary, $\varepsilon(k)$ may not be stationary. There is, thus, the need to look for a procedure for stationarizing the signal in (30) such that the deterministic signal would be associated with a stationary noise which would be further analysis easier. The method used here is the same as the one used in [10]. The resulting stationary signal is therefore

$$\hat{X}(k) = \sum_{i=1}^{M} B_i e^{\left(j\frac{2\pi k}{N_d}\ln \lambda_i\right)} + e(k) \qquad (31)$$

$k = 1, 2, \ldots, N_d$; $N_d = 2N_0 + 1$, N_0 is the truncation point and $e(k)$ is the new stationary white noise.

The noisy sum of complex exponentials in (31) is further processed using an autoregressive moving average (ARMA) model whose AR parameters are determined by solving high-order Yule-Walker equations (HOYWE) via singular value decomposition (SVD). This is achieved by considering the deconvolved and truncated data to be the output of an ARMA model whose input is a complex white noise sequence $e(k)$ so that

$$\sum_{n=0}^{p} a_n x(k-n) = \sum_{n=0}^{q} b_n e(k-n), \qquad a_0 = 1 \qquad (32)$$

where a_n and b_n represent respectively the AR and moving average (MA) model coefficients and p and q are AR and MA model orders respectively.

The remaining procedure is as detailed in [3]. The guess values of the AR and MA model order are respectively p_e and q_e and the desired power distribution of $x(t)$ denoted as $P_x(t)$ is obtained as follows:

$$P_x(t) = S_f(z)\Big|_{z=\exp\left(\frac{j2\pi}{N\Delta t}\right)} = \sum_{k=1}^{M} B_k^2 \delta(t - \ln \lambda_k) \qquad (33)$$

IV. SIMULATION RESULTS

In this section, simulation results are presented. These simulations are carried out to investigate the efficacy of the methods proposed in this paper. First, the truncation point was established using CRLB. Simulations were then carried out to establish the following:

- Resolvability of the exponents.
- The response of the proposed technique using a high resolution signal.
- The ability of the method to resolve signals with large number of components of diversified magnitudes.
- Effect of deconvolution parameters.

A. Determination of the Truncation Point

The truncation point, N_0 is critical to the performance of any technique to be used to process the deconvolved data, $\hat{x}$. CRLB being a good measure of the efficiency of parameter estimates has been used to establish the quality of the parameter estimates for different values of N_0. By varying the data length and comparing of the resulting estimates with the CRLB we can know which data length would produce the best estimator. Derivation of the CRLB was done as presented in [6]. The signal used for this simulation is

$$\begin{aligned} S(\tau) = 50e^{-0.025\tau} + 100e^{-0.1\tau} \\ + 200e^{-0.2\tau} + 350e^{-0.7\tau} + n(\tau) \end{aligned} \qquad (34)$$

The reasons for the choice of this signal were given in [10]. Simulations using the proposed ARMA algorithm with conventional inverse filtering showed that the spectrum is good only for $27 \le N_0 \le 33$ with the best performance at $N_0 = 27$.

B. Resolvability of the Components

To investigate the capability of the proposed combination to analyze basic signals, the following two-component signal was used:

$$S_1(\tau) = 0.1e^{-0.1\tau} + 0.2e^{-0.2\tau} \qquad (35)$$

The distribution function is:

$$x_1(t) = 0.1^{(1-\alpha)}\delta(t - \ln 10) + 0.2^{(1-\alpha)}\delta(t - \ln 5) \qquad (36)$$

The signal was synthesized in MATLAB with noise added using the function *awgn* which is an embedded MATLAB function. Table II shows the result of applying the proposed combination over low ($SNR \le 40dB$), medium ($40dB < SNR < 100dB$) and high ($SNR \ge 100dB$)

SNRs. A plot of the distribution function for high SNR is shown in Fig. 1. The distribution function was plotted against negative time in order to arrange the exponents in ascending order on the horizontal axis. For the purpose of comparison, DFT plot is shown (broken lines) along with the actual plot (solid). The DFT graphs are obtained by windowing the deconvolved data to remove high frequency noise and then inverse transforming, instead of using SVD-ARMA or any other parametric modelling technique. The results are based on $p_e = 20$, $q_e = 5$ and the choice of deconvolution parameters is according to Table I.
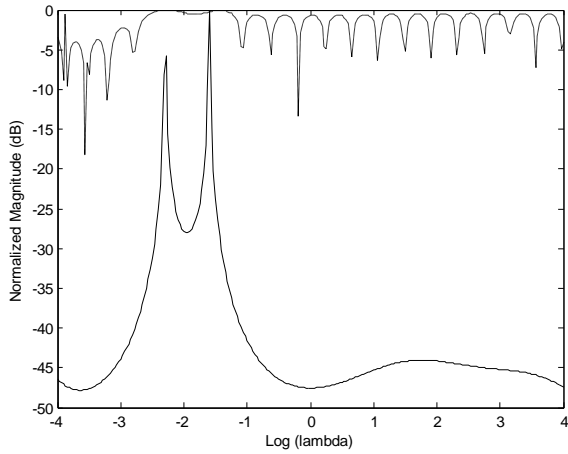

Fig. 1. Power distribution for $x_1(t)$ at a medium SNR

TABLE I: RECOMMENDED DECONVOLUTION PARAMETERS

Parameter	SNR		
	Low	Medium	High
ς (dB)	-20	-40	-80
γ (dB)	-100	-100	-100

TABLE II: ESTIMATED LOG OF DECAY RATES ($\ln \lambda_i$) FOR $S_1(\tau)$

Expected Value	LOW SNR	MEDIUM SNR	HIGH SNR
-2.3025	-2.531	-2.41	-2.28
-1.6094	-1.708	-1.68	-1.561

C. Response to a High Resolution Signal

The following signal was used to test the effectiveness of the proposed combination in resolving a high resolution signal.

$$S(\tau) = 0.5e^{-0.5\tau} + e^{-\tau} + 2e^{-2\tau} \\ + 5e^{-5\tau} + 10e^{-10\tau} + n(\tau) \tag{37}$$

It is noteworthy that for this signal $\dfrac{\lambda_1}{\lambda_2} = \dfrac{\lambda_2}{\lambda_3} = \dfrac{\lambda_4}{\lambda_5} = \dfrac{1}{2}$.

Analysing this signal would prove difficult if conventional methods like Prony, nonlinear least squares, etc. are used.

The distribution function for the signal $S_2(\tau)$ is as follows:

$$x_2(t) = 0.5^{(1-\alpha)}\delta(t - \ln 2) + \delta(t) + 2^{(1-\alpha)}\delta(t + \ln 2) \\ + 5^{(1-\alpha)}\delta(t + \ln 5) + 10^{(1-\alpha)}\delta(t + \ln 10) \tag{38}$$

The result of applying the proposed combination on $S(\tau)$ is shown in Table III. Fig. 2 shows a typical power distribution for $x_2(t)$. It is observed that while the combination gives good results over medium and low SNR, it yields poor estimates at low SNRs.

TABLE III: ESTIMATED LOG OF DECAY RATES ($\ln \lambda_i$) FOR $S_2(\tau)$

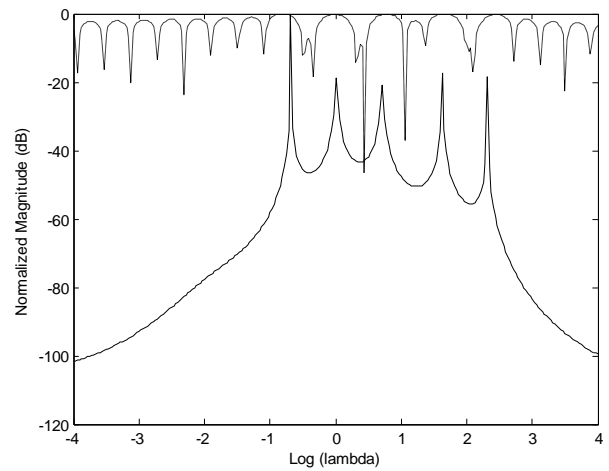| Expected Value	LOW SNR	MEDIUM SNR	HIGH SNR
-0.6931	POOR	-0.7813	-0.75
0	RESULTS	-0.0625	0.0312
0.6931		0.75	0.75
1.6094		1.625	1.594
2.3025		3.375	2.406

Fig. 2. Power distribution for $x_2(t)$ at high SNR using SVD-ARMA with MPD

D. Ability to Resolve Signals with Large Number of Components

Also tested is the ability of the combination to resolve large number of components of diversified magnitude. To achieve that, the following signal is used:

$$S_3(\tau) = 0.01e^{-0.01\tau} + 0.025e^{-0.025\tau} \\ + 0.05e^{-0.05\tau} + 0.1e^{-0.1\tau} + 0.5e^{-0.5\tau} \tag{39} \\ + 2e^{-2\tau} + 10e^{-10\tau} + 25e^{-25\tau} + n(\tau)$$

The distribution function for this signal is

$$x_3(t) = 0.01^{(1-\alpha)}\delta(1 - \ln 100) + 0.025^{(1-\alpha)}\delta(1 - \ln 40) + 0.1^{(1-\alpha)}\delta(1 - \ln 20) \tag{40} \\ + 0.1^{1-\alpha}\delta(1 - \ln 10) + 0.5^{(1-\alpha)}\delta(1 - \ln 2) + 2^{(1-\alpha)}\delta(1 + \ln 2) \\ + 10^{(1-\alpha)}\delta(1 + \ln 10) + 25^{(1-\alpha)}\delta(1 + \ln 25)$$

Table IV shows the result of applying our combination to this signal. All the components are detected over high SNR, but poor results are obtained over low and medium SNRs. A typical distribution function of $x_3(t)$ is shown in Fig. 3.

Table V shows typical singular values obtained from simulations for $S_1(\tau)$, $S_2(\tau)$ and $S_3(\tau)$. The number of components M can always be obtained by observing the number of singular values that are significant.

TABLE IV: ESTIMATED LOG OF DECAY RATES ($\ln \lambda_i$) FOR $S_2(\tau)$

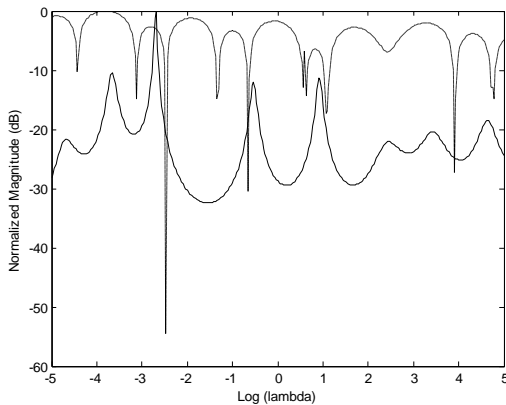| Expected Value	LOW SNR	MEDIUM SNR	HIGH SNR
-4.6052	POOR RESULTS	POOR RESULTS	-4.2190
-3.6888			-3.1560
-2.9957			-2.3130
-2.3025			-0.6875
-0.6931			-0.7188
0.6931			2.3440
2.3025			3.2500
3.2188			4.8440

Fig. 3. Power distribution for $x_3(t)$ at a high SNR using SVD-ARMA

TABLE V: TYPICAL SINGULAR VALUES OBTAINED FROM SIMULATIONS FOR $S_1(\tau)$, $S_2(\tau)$ AND $S_3(\tau)$

Singular values for $S_1(\tau)$ (MPD)	Singular values for $S_2(\tau)$ (MPD)	Singular values for $S_3(\tau)$ (MPD)
44.641	53.735	54.022
5.1023	45.07	32.159
6.3874e-015	18.703	28.771
3.4092e-015	1.9548	23.31
1.9057e-015	0.12072	22.205
1.6265e-015	1.172e-014	12.94
1.4692e-015	8.798e-015	6.8497
1.2536e-015	3.9246e-015	0.18479
1.1585e-015	3.5549e-015	1.0118e-014
9.921e-016	3.1613e-015	8.0858e-015
8.6774e-016	2.2697e-015	5.7101e-015
7.8747e-016	2.1729e-015	3.9679e-015
7.0679e-016	2.0247e-015	3.4256e-015
6.7509e-016	1.7994e-015	2.8723e-015
5.1244e-016	1.6101e-015	2.3961e-015
4.5115e-016	1.3916e-015	2.144e-015
3.931e-016	1.0135e-015	1.7892e-015
3.106e-016	8.3472e-016	1.492e-015
2.4038e-016	6.2773e-016	1.1756e-015
1.5872e-016	4.3248e-016	1.0962e-015

E. Effect of Variation of Deconvolution Parameters

The multiparameter deconvolution filter was developed to overcome the errors caused by the straightforward division used in conventional inverse filtering in the frequency domain. The deconvolution parameters control the balance between the degree of noise reduction and the errors introduced by the filters. Setting them to zero maximizes the deconvolution noise while making their values high introduces error in the estimate. Several simulations are needed to establish an optimal combination of these parameters. The simulations were carried out over the three different ranges of SNR (low, medium and high) using the

test signal of (34) whose distribution function is (with $\alpha = 0.5$):

$$x(t) = 316\delta(t - \ln 40) + 316\delta(t - \ln 10) + 447\delta(t - \ln 5) + 418\delta(t + \ln 0.7) \tag{41}$$

Several simulations were carried out using different combinations of β and γ which lead to the recommended values of the deconvolution parameters in Table I.

V. EXPERIMENTAL RESULTS

The combination proposed in this paper was used to postprocess real data obtained from a mixture of Acridine orange and quinine using a spectrofluorometer. The experimental setup is shown in Fig. 4. The data generated by the spectrofluorometer is collected by the PC (as in this case) or fed to another digital signal processing unit for further processing using the proposed combination.
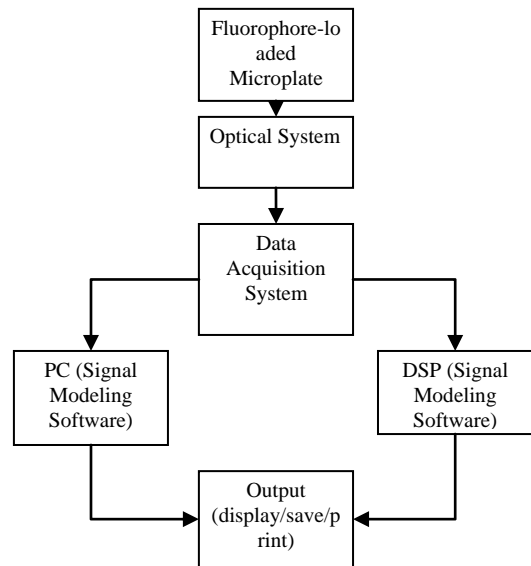

Fig. 4. Experimental setup for fluorescence decay analysis.

The proposed combination was applied to the data in a similar manner done in the simulation. Here, α was selected to be 0.5. The deconvolution parameters were selected as for medium SNR as given in Table I. The sampling interval was 0.25 and $n_{\max} = 44$, $n_{\min} = -83$, making $N = 128$. The results are based on $p_e = 20$, $q_e = 5$.

Table VI shows the estimated log of decay rates for the three cases of Acridine orange, Quinine and a mixture of the two. The power distributions are shown in Fig. 5, Fig. 6 and Fig. 7.

TABLE VI: ESTIMATED LOG OF DECAY RATES ($\ln \lambda_i$) FROM FLUORESCENCE DECAY EXPERIMENTS.

Mixture	Expected value	Log estimates	Percentage deviation
Acridine orange	0.5978	0.625	4.55
Quinine	-0.6419	-0.625	2.63
Acridine Orange +Quinine	0.7750	0.75	0.37
	-0.5539	-0.5313	0.73

Looking at the table, it is obvious that the resolving power of the proposed method is very good even for practical signals. It can also be observed that the level of noise is relatively very low by virtue of percentage deviation and the shapes of the power distribution curves in Figures 5 through Fig. 7.
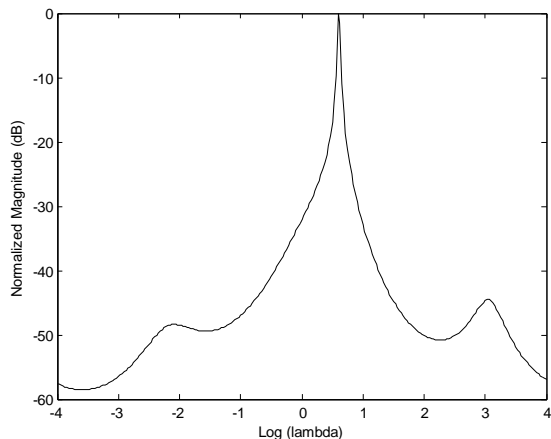
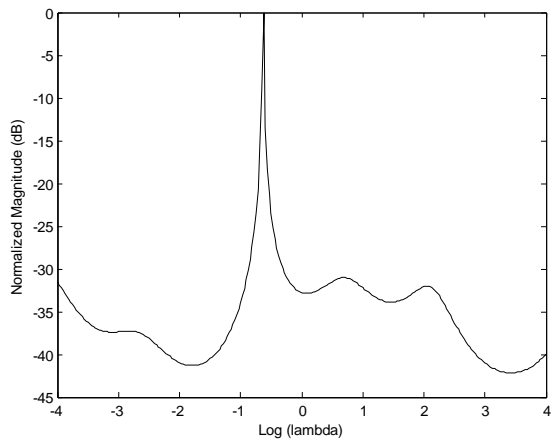Fig. 5. Power distribution for acridine orange in water

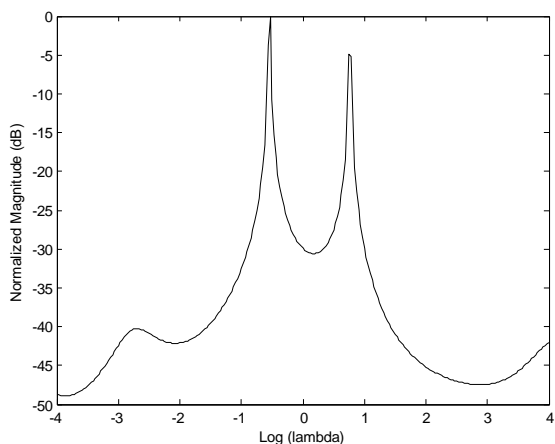Fig. 6. Power distribution for quinine in water

Fig. 7. Power distribution for quinine + acridine orange in water

VI. CONCLUSION

In this paper and enhanced method is proposed for the analysis of transient multiexponential signals. Based on the Gardner transform, the method combines multiparameter deconvolution and ARMA modeling technique to analyse this class of signals. The method has been shown to be able to resolve basic signals for even very low SNR and high resolution signals and signals with large number of components over medium and high SNRs.

The major drawback of the method is the fact that deconvolved data has to be truncated at a point which in this paper was determined using Cramer Rao Lower Bound (CRLB).

REFERENCES

[1] A. A. Istratov and O. F. Vyvenko, "Exponential Analysis in Physical Phenomena," *Rev. Sci. Instruments.*, vol. 70 no. 2, pp. 1233-1257, 1999.

[2] A. U. Jibia and M. J. E. Salami, "An appraisal of gardner transform-based methods of transient multiexponential signal analysis," *International Journal of Computer Theory and Engineering*, 2012, vol. 4, no. 1, pp. 16-25.

[3] M. J. E. Salami and. N. Sidek, "Parameter estimation of multicomponent transient signals using deconvolution and ARMA modeling techniques," *Journal of Mechanical Systems and Signal Processing*, vol. 17, no. 6, pp. 1201 - 1218, 2003.

[4] T. Daboczi and I. Kollár, "Multiparameter optimization of inverse filtering algorithms," *IEEE Transactions on Instrumentation and Measurement,* vol. 45, no. 2, pp. 417-421, 1996.

[5] Z. Zhang, D. Wang, W. Wenlian, H. M. Du, and J. Zu, "A group of inverse filters based on stabilized solutions of fredholm integral equations of the first kind," *IEEE International Instrumentation and Measurement Technology Conference Victoria*, Vancouver Island, Canada, May 12-15, 2008, pp. 668 – 671.

[6] A. U. Jibia, M. J. E. Salami, O. O. Khalifa, and F. A. M. Elfaki, "Cramer-rao lower bound for parameter estimation of multiexponential signals," *Proceedings of 16th International Conference on Systems, Signals and Image Processing (IWSSIP 2009)*, Chalkida, Greece. 2009, pp. 1-5.

[7] A. U. Jibia and M. J. E. Salami, "Transient Multiexponential Data Selection Using Cramer-Rao Lower Bound," *Proc. International Conference on Computer and Automation Engineering, Mumbai*, January 2012, pp. 227-232.

[8] D. G. Gardner, J. C. Gardner, G. Lush, and W. R. Ware, "Method for the analysis of multicomponent exponential decay curves," *Journ. Chem. Phys.*, vol. 31, pp. 978-986, 1959.

[9] M. J. E. Salami, "Application of ARMA models in multicomponent signal analysis," *Ph.D. Dissertation*, Dept. of Electrical Engineering, University of Calgary, Calgary, Canada, 1985.

[10] A. U. Jibia and M. J. E. Salami, "Analysis of transient multiexponential signals using exponential compensation deconvolution," *Measurement* vol. 45, pp. 19–29, 2012.